

Spin wave modes in magnetic nanodisks under in-plane magnetic field

T. Kaneko,¹ S. M. Noh,² K. Miyake,² M. Sahashi,² and H. Imamura^{1,2,*}

¹*Nano-scale theory group, NRI, AIST, Tsukuba, Ibaraki, 305-8568, Japan*

²*Department of Electronic Engineering, Tohoku University, Sendai 980-8579 Japan*

(Dated: March 1, 2012)

The size dependence of spin wave modes in a circular Permalloy (Py) nanodisk under an in-plane magnetic field is systematically studied by using micromagnetics simulations. We show that as the disk diameter is increased, the resonance frequency of the backward mode decreases while that of the uniform mode increases. The avoided crossing of resonance frequencies of the uniform mode and the backward mode appears in the plot of the size dependence of resonance frequencies and the backward mode turns into the so-called “edge mode” for large nanodisks.

PACS numbers: 75.78.-n, 75.75.Jn, 76.50.+g

The dynamics of magnetizations confined in a magnetic nanostructure is of special interest due to emerging applications in spintronics devices, such as future recording head sensors, magnetic random-access memories and spin torque oscillators.¹ Ferromagnetic resonance (FMR) measurement is a powerful tool to investigate the high-frequency response of magnetizations. When magnetization is confined in a nanoscale structure, the FMR spectra of the magnetic nanostructures show multi-peaks, i.e., several spin wave modes are excited.^{2,3}

The spin wave modes of in-plane magnetized film are classified into two modes depending on the relative direction of the magnetization vector at equilibrium, \mathbf{M}_0 , and the wavevector of the spin wave, \mathbf{q} .^{4,5} One is the Damon and Eshbach (DE) mode where \mathbf{q} is perpendicular to \mathbf{M}_0 .⁴ The other is the backward (BA) mode where \mathbf{q} is parallel to \mathbf{M}_0 .⁵ These two modes have been observed in magnetic wires using Brillouin light scattering (BLS).^{6,7} For magnetic nanostructures, another spin wave mode called the “edge mode”, where the spin wave is localized around edges, appears. The edge mode has been observed in thin films,^{8,9} wires, circular disks^{10–13} and elliptic disks.^{14–17} It is important to study the relation among these spin wave modes in magnetic nanostructures from both scientific and practical points of view.

In this paper, we systematically investigated the size dependence of spin wave modes in the magnetic nanodisk shown in Fig. 1 (a) by using micromagnetics simulations. Until now it has been widely accepted that the origin of the edge mode is the pinning of the spin wave due to the strong demagnetization field around the edges and that the edge mode has no relation with the BA or DE modes.^{8,9} However, we show that the edge mode can be regarded as the BA mode with two nodes.

In order to solve the Landau-Lifshitz-Gilbert (LLG) equation for a circular Py disk with thickness $h = 10$ nm under an in-plane magnetic field we employed NMAG code^{18,19} which is a micromagnetics simulation package based on the finite-element and boundary-element methods. We assumed a saturation magnetization of $M_s = 0.8 \times 10^6$ A/m, an exchange stiffness is $A = 1.3 \times 10^{-11}$ J/m and a Gilbert damping constant of $\alpha = 0.01$. The finite element mesh was generated us-

ing Gmsh.²⁰ The size of the mesh was about 5 nm and we confirmed that this mesh was sufficiently fine to describe the spin wave dynamics of the magnetic nanodisk we considered. The static magnetic field, $\mathbf{H}_{\text{ext}} = H_{\text{ext}}\mathbf{e}_y$, was applied in the y -direction and the oscillating magnetic field, $\mathbf{h}_{\text{rf}} = h_{\text{rf}} \sin(2\pi ft)\mathbf{e}_x$, of frequency f was applied in the x -direction as shown in Fig. 1 (a). We assumed

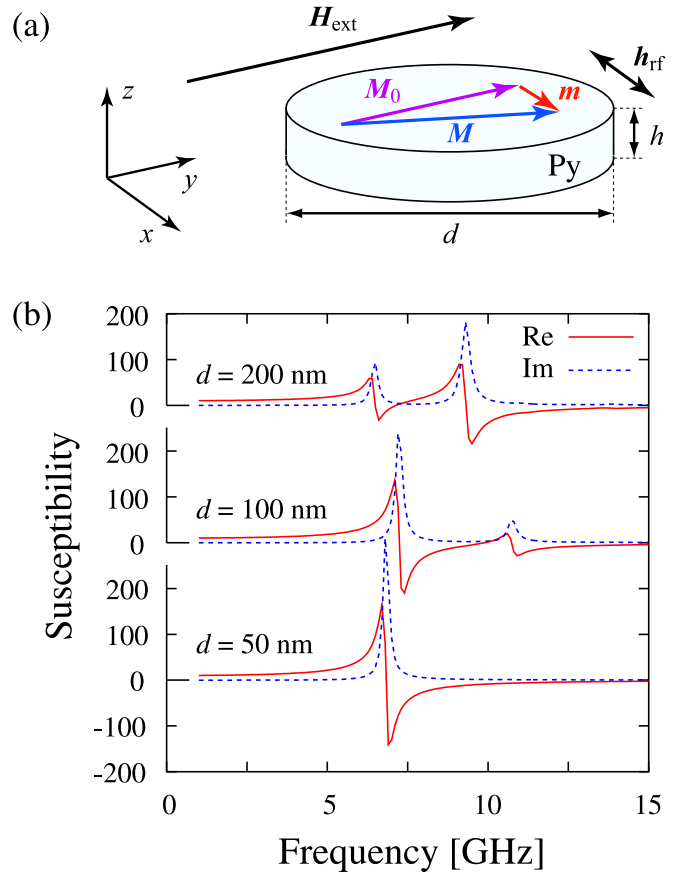


FIG. 1. (Color online) (a) Schematic illustration of a circular Py nanodisk under static \mathbf{H}_{ext} and oscillating \mathbf{h}_{rf} magnetic fields. (b) Real and imaginary parts of the calculated complex susceptibilities are plotted by the dotted and solid lines, respectively, for $d=50, 100$ and 200 nm.

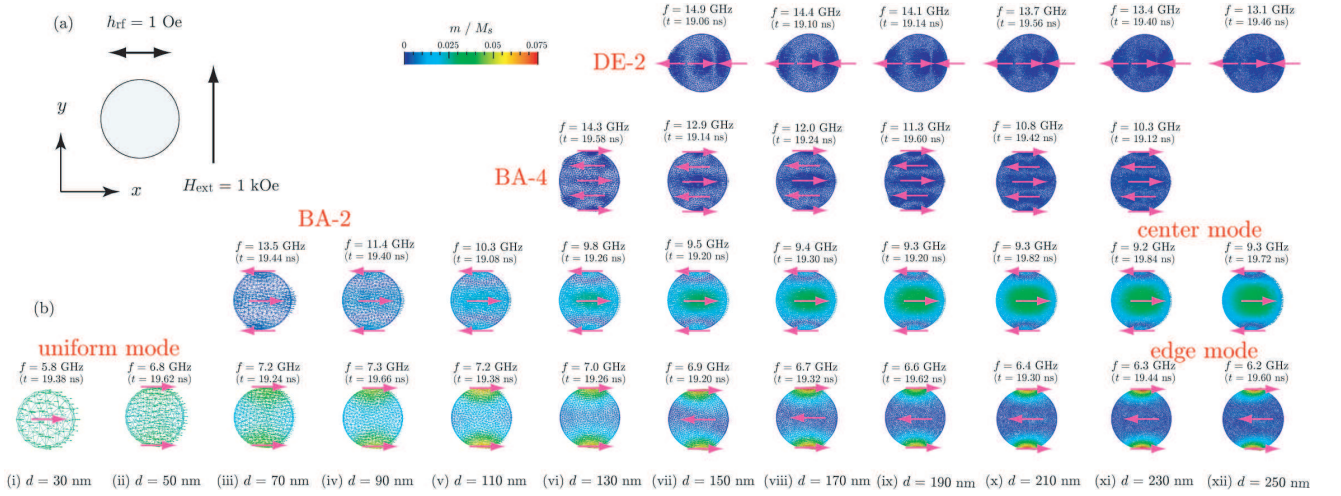


FIG. 2. (Color online) (a) Directions of the static and oscillating magnetic fields are shown. (b) Snapshots of the distribution of the deviation, $\mathbf{m}(\mathbf{r}, t)$, in a nanodisk with $d = 30$ nm (i), 50 nm (ii), 70 nm (iii), 90 nm (iv), 110 nm (v), 130 nm (vi), 150 nm (vii), 170 nm (viii), 190 nm (ix), 210 nm (x), 230 nm (xi) and 250 nm (xii). The pink arrows indicate the directions of the deviation, $\mathbf{m}(\mathbf{r}, t)$, at the anti-nodes. The labels BA- n and DE- n stand for the BA and DE modes with n nodal surfaces.

$H_{\text{ext}} = 1.0$ kOe and $h_{\text{rf}} = 1$ Oe. We obtained a single domain state as an equilibrium magnetization configuration for nanodisks with $d \leq 250$ nm. Starting with the equilibrium magnetization configuration we calculated the time evolution of the magnetization $\mathbf{M}(\mathbf{r}, t)$ for 20 ns under the in-plane magnetic field of $\mathbf{H}_{\text{ext}} + \mathbf{h}_{\text{rf}}(t)$.

We introduce the deviation of the magnetization defined as $\mathbf{m}(\mathbf{r}, t) = \mathbf{M}(\mathbf{r}, t) - \mathbf{M}_0(\mathbf{r})$, where $\mathbf{M}_0(\mathbf{r})$ is the equilibrium magnetization. The deviation $\mathbf{m}(\mathbf{r}, t)$ represents the amplitude of a spin wave excited by an oscillating magnetic field. The real and imaginary part of the complex susceptibility χ was obtained by fitting the average of the x -component of the deviation, \overline{m}_x , to

$$\overline{m}_x = \text{Re}(\chi)h_{\text{rf}}\sin(2\pi ft) - \text{Im}(\chi)h_{\text{rf}}\cos(2\pi ft), \quad (1)$$

after the oscillation was stabilized. In Fig. 1 (b) we plot the real and imaginary part of χ by the solid and dotted lines, respectively for $d=50, 100$ and 200 nm. The resonance frequencies were 6.8 GHz for $d = 50$ nm, 7.2 and 10.7 GHz for $d = 100$ nm and 6.5, 9.3, 11.0 and 13.8 GHz for $d = 200$ nm. For $d = 200$ nm, the magnitudes of χ at 11.0 and 13.8 GHz were so small that we used log-scale plots to identify them. The calculated resonance frequencies were in good agreement with those observed in TR-MOKE measurement of circular Py nanodisks with $h = 10$ nm by Shaw *et al.* They observed about 7 GHz for $d = 50$ nm, 7 and 10 GHz, for $d = 100$ nm, and 7 and 9 GHz for $d = 200$ nm under the in-plane magnetic field of 1 kOe¹³.

Figure 2 (b) shows snapshots of the deviation, $\mathbf{m}(\mathbf{r}, t)$, at the resonance frequencies for $d = 30, 50, \dots, 250$ nm. The directions of the static and oscillating magnetic fields in this plot are shown in Fig. 2 (a). The labels BA- n and DE- n stand for the BA and DE modes with n nodal surfaces as shown in Fig. 2 (b). The pink arrows indicate

the directions of the deviation, $\mathbf{m}(\mathbf{r}, t)$, at the anti-nodes. We could not identify the third lowest mode for $d = 250$ nm since its resonance frequency was very close to that of the center mode. For $d = 30$ nm, the deviation, \mathbf{m} , was uniformly distributed throughout the disk, i.e., the uniform mode was excited.²¹ As the disk diameter, d , is increased, other resonant spin wave modes classified as BA-2, BA-4 and DE-2 modes appear. It should be noted that for a large nanodisk the lowest mode is not the uniform mode but the edge mode, and the second lowest mode is not the BA-2 mode but the center mode. Tracing the spin wave modes of the lowest-resonance frequencies, i.e., the bottom line of Fig. 2 (b), one might come up with the idea that the origin of the edge mode is the uniform mode and it has no relation with either the BA or DE modes. However, our systematic investigation of the resonant spin wave modes revealed that the above interpretation is not valid.

In Fig. 3 we plot the size dependence of the calculated resonance frequencies by circles with radii proportional to the imaginary part of the susceptibility, $\text{Im}(\chi)$. The blue dotted lines are visual guides connecting resonance frequencies in the same branches. The purple solid line represents the resonance frequencies given by the Kittel equation²¹:

$$f_K = \sqrt{f_H(f_H + (N_z - N_y)f_M)}, \quad (2)$$

where $f_H = \gamma H_{\text{ext}}/2\pi$, $f_M = \gamma M_s/2\pi$, γ is the gyromagnetic ratio and N 's represent the demagnetization factors estimated by means of the micromagnetics simulations. For small nanodisks with $d \leq 60$ nm, we obtained a single resonance peak at frequencies close to those given by the Kittel equation of Eq. (2). As the disk diameter, d , is increased, the frequency of the uniform mode increases due to the increase of the demagnetization field, while those

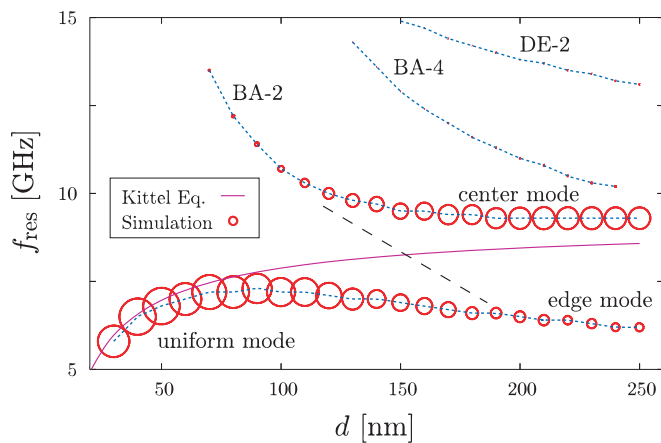


FIG. 3. (Color online) Calculated resonance frequencies, f_{res} , are plotted by circles with radii proportional to imaginary part of the susceptibility, $\text{Im}(\chi)$, against the disk diameter, d . The blue dotted lines are visual guides connecting resonance frequencies in the same branches. The purple solid line represents the resonance frequencies given by the Kittel equation of Eq. (2). The labels of the excited spin wave modes are the same as those in Fig. 2 (b).

of the BA-2, BA-4 and DE-2 modes decrease. At around $d \simeq 150$ nm where the frequency of the BA-2 mode comes close to that of the uniform mode, an avoided crossing of the BA-2 mode and uniform mode appears and the BA-2 mode becomes the edge mode for large disks as indicated by the black dashed line. Therefore, the edge mode can be regarded as the BA-2 mode with two nodes. The uniform mode becomes the center mode, the frequency of which is close to that given by the Kittel equation.

In summary, we investigated the size dependence of spin wave modes in a circular Py nanodisk with $d \leq 250$ nm under an in-plane magnetic field using micromagnetics simulations. We showed that the excited spin wave modes are classified into uniform mode, edge mode, center mode, BA-2 mode, BA-4 mode, and DE-2 mode depending on the size of the nanodisk. For large disks, we found an avoided crossing of the BA-2 and uniform modes, at which BA-2 mode (uniform mode) becomes the edge mode (center mode).

The authors acknowledge M. Doi and H. Arai for valuable discussions. This work was supported in part through NEDO, the Storage Research Consortium (SRC) and Center of Education, Research for Information Electronics Systems of Global COE Program, and MEXT.

* h-imamura@aist.go.jp

- ¹ J. W. Lau and J. M. Shaw, J. Phys. D: Appl. Phys. **44**, 303001 (2011).
- ² L. R. Walker, J. Appl. Phys. **29**, 318 (1958).
- ³ S. Noh, D. Monma, K. Miyake, M. Doi, T. Kaneko, H. Imamura, and M. Sahashi, IEEE Trans. Magn. **47**, 2387 (2011).
- ⁴ R. Damon and J. Eshbach, J. Appl. Phys. **31**, 104S (1960).
- ⁵ B. A. Kalinikos and A. N. Slavin, J. Phys. C **19**, 7013 (1986).
- ⁶ J. Jorzick, S. O. Demokritov, C. Mathieu, B. Hillebrands, B. Bartenlian, C. Chappert, F. Rousseaux, and A. N. Slavin, Phys. Rev. B **60**, 15194 (1999).
- ⁷ C. Mathieu, J. Jorzick, A. Frank, S. O. Demokritov, A. N. Slavin, B. Hillebrands, B. Bartenlian, C. Chappert, D. Decanini, F. Rousseaux, and E. Cambril, Phys. Rev. Lett. **81**, 3968 (1998).
- ⁸ M. Bailleul, D. Olligs, C. Fermon, and S. O. Demokritov, Europhys. Lett. **56**, 741 (2001).
- ⁹ J. Jorzick, S. O. Demokritov, B. Hillebrands, M. Bailleul, C. Fermon, K. Y. Guslienko, A. N. Slavin, D. V. Berkov, and N. L. Gorn, Phys. Rev. Lett. **88**, 047204 (2002).
- ¹⁰ G. Gubbiotti, G. Carlotti, T. Okuno, T. Shinjo, F. Nizzoli, and R. Zivieri, Phys. Rev. B **68**, 184409 (2003).

- ¹¹ L. Giovannini, F. Montoncello, F. Nizzoli, G. Gubbiotti, G. Carlotti, T. Okuno, T. Shinjo, and M. Grimsditch, Phys. Rev. B **70**, 172404 (2004).
- ¹² I. Neudecker, K. Perzlmaier, F. Hoffmann, G. Woltersdorf, M. Buess, D. Weiss, and C. H. Back, Phys. Rev. B **73**, 134426 (2006).
- ¹³ J. M. Shaw, T. J. Silva, M. L. Schneider, and R. D. McMichael, Phys. Rev. B **79**, 184404 (2009).
- ¹⁴ G. Gubbiotti, G. Carlotti, T. Okuno, M. Grimsditch, L. Giovannini, F. Montoncello, and F. Nizzoli, Phys. Rev. B **72**, 184419 (2005).
- ¹⁵ J. Jersch, V. E. Demido, H. Fuchs, K. Rott, P. Krzysteczko, J. Münchenberger, G. Reiss, and S. O. Demokritov, Appl. Phys. Lett. **97**, 152502 (2011).
- ¹⁶ L. Giovannini, F. Montoncello, F. Nizzoli, P. Vavassori, and M. Grimsditch, Appl. Phys. Lett. **99**, 186191 (2011).
- ¹⁷ H. T. Nembach, J. M. Shaw, T. J. Silva, W. L. Johnson, S. A. Kim, R. D. McMichael, and P. Kabos, Phys. Rev. B **83**, 094427 (2011).
- ¹⁸ T. Fischbacher, M. Franchin, G. Bordignon, and H. Fangohr, IEEE Trans. Magn. **43**, 2896 (2007).
- ¹⁹ <http://nmag.soton.ac.uk/nmag/>.
- ²⁰ <http://www.geuz.org/gmsh/>.
- ²¹ C. Kittel, Phys. Rev. **73**, 155 (1948).